Fusion-fission dynamics at high excitation energies studied by neutron emission

W. P. Zank, D. Hilscher, G. Ingold, U. Jahnke, M. Lehmann, and H. Rossner
Hahn-Meitner-Institut für Kernforschung Berlin, 1000 Berlin 39, Federal Republic of Germany
(Received 12 September 1985)

Neutron emission in coincidence with fusion-fission events and evaporation residues was measured in the heavy-ion reactions ^{141}Pr+(316 MeV)^{40}Ar and ^{175}Lu+(192 MeV)^{12}C. Both reactions are leading to similar composite systems and excitation energies as the previously investigated reaction ^{165}Ho+^{20}Ne. In order to determine the lifetimes of the composite systems prior to scission and to study entrance channel and angular-momentum effects, the results for all three systems are compared. From measured cross sections of fission and evaporation residues, the angular momentum intervals leading to fission are deduced to be 50–109 $\hbar$ and 49–62 $\hbar$ for Pr+Ar and Lu+C, respectively. The corresponding prescission neutron multiplicities are deduced to be $M_n^{presc}=3.6\pm0.6$ and 6.3 ± 0.8, whereas the respective postscission multiplicities are $M_n^{post}=4.4\pm0.4$ and 3.6 ± 0.6. For the system ^{175}Lu+^{12}C it is found that 0.5 ± 0.2 preequilibrium neutrons are emitted. In contrast to the evaporative neutrons, a strong anisotropy $a_n^{PE}=2.2\pm0.6$ relative to the reaction plane defined by one fission fragment and the beam direction is observed. From the prescission neutron multiplicities, the evaporation time of the system prior to scission is deduced using the statistical model to $\approx(3-12)\times10^{-20}$ s. Nucleus deformation effects and neutron emission from not fully accelerated fission fragments are taken into account. The unexpected long prescission lifetimes can be explained as long transition times to the scission point caused by a large two-body viscosity. Under this assumption the viscosity parameter of the highly excited nuclei has been determined in a first approximation to $\mu\approx0.1$ TP. The results might be understood also assuming a mixture of a two-body and one-body friction.

I. INTRODUCTION

The dynamics of fission under extreme conditions, such as high temperatures and angular momenta, is a most interesting and yet unsolved problem in one of the oldest topics of nuclear physics and chemistry. It provides an excellent testing ground for nuclear many-body theories such as dissipation mechanisms and viscosity of nuclear matter as a function of temperature. In the present investigation the dynamics of fission is studied as a function of angular momentum by means of the transition time of a fissioning nucleus on its way to the scission point. This time is deduced from the number of neutrons evaporated from the composite system prior to scission.

Experimentally,[1–8] as well as theoretically,[9–12] heavy-ion induced fission has received, in recent years, considerable attention by many investigators. The angular distributions of fission fragments are essentially symmetric to 90° and consequently a long-lived equilibrated composite system must exist with lifetimes longer than one rotation time at least for asymmetric systems.[13] This time can be used to yield only a lower limit for the lifetime of the composite system if we know the equilibrium shape and thus the respective moments of inertia. A better means to deduce lifetimes of composite systems is to measure the number of evaporated light particles. Experimentally, these particles have to be separated from those emitted from the partially or fully accelerated fission fragments. This is done by employing the spatial correlation of light-particle yield in the laboratory frame with the direction and magnitude of the velocity vectors of either the composite system or the two fully accelerated fission fragments. This technique was already extensively used to determine the prefission neutrons from multiple-chance fission in light-ion induced fission.[14,15] Provided that we know the particle decay widths as a function of temperature, we can associate with the measured number of light particles an evaporation time and thus a lifetime of the composite system. Whereas the dynamics of fission is deduced from the number of light particles which are evaporated *after* the system has decided to fission and moves towards the scission point. The true prefission light-particle multiplicity of multiple-chance fission contains[14,15] only static information on the relative phase space for fission and light-particle evaporation. In the following we will refer to light particles evaporated prior to scission as prescission particles.

In heavy-ion induced fission a considerable amount of cross section can be due to partial waves larger than the angular momentum at which the fission barrier vanishes.[16,17] In this case the final exit channel will consist of two fragments independent of the number of evaporated light particles. For such a system the light particle emission does not compete with, but rather accompanies fission until the system reaches the scission point.

The fusion time depends very strongly on the mass asymmetry of the initial two fragments. For systems with small mass asymmetry as Ho + Ar, Grégoire *et al.*[9] predict fusion times in the order of $(1-3)\times10^{-20}$ s. Such long times are consistent with the experimental findings that in such systems a considerable amount of charged particles, in particular α particles, were observed.[6–8] For instance Schad *et al.*[6] deduced for the systems Ag + Cl a lifetime of $(1-3)\times10^{-20}$ s. However, for systems where

the mass asymmetry of projectile and target such as Ho + Ne is larger, and thus the theoretical fusion time (10^{-21} s) is smaller, unexpectedly large prescission neutron multiplicities[1-5] were observed. The deduced lifetimes were also in the order of $(2-4)\times 10^{-20}$ s (Ref. 3). Measured prescission neutron multiplicities are at least a factor of 20 to 50 larger than the observed α-particle multiplicities due to Coulomb barrier effects. The multiplicities and spectral shapes of emitted α particles sensitively depend also on the deformation and angular momentum of the composite system. This can yield, of course, additional information such as shielding effects of emitted particles by the two fission fragments in close proximity,[6] but can also be a disadvantage in deducing nuclear temperatures and calculating decay widths for charged particles. These problems do not exist for neutron emission which is essentially independent from the shape degree of freedom and does not show any anisotropy with respect to the spin of the composite system as does the α-particle emission.[6]

The present investigation was undertaken to provide systematic data on prescission neutron emission from almost the same composite system at the same excitation energy but different entrance channel mass asymmetries, and in particular for different angular momenta. To this purpose we have studied in addition to the previously investigated system Ho + Ne (Ref. 3) the systems Pr + Ar and Lu + C leading to ^{185,181,187}Ir, respectively, at an excitation energy of 164 MeV assuming complete fusion. In order to study in detail anisotropies with respect to the spin direction of the fissioning nucleus special geometries were chosen in the present investigation. In order to provide also the necessary information for interpretation of the data the inclusive angular distributions of fission fragments and evaporation residues were measured. In Sec. II the experimental procedure is briefly described, in Sec. III the data analysis and the results are presented, and in Sec. IV the lifetimes of the composite systems are deduced from the present data employing various assumptions on nuclear dissipation mechanisms.

II. EXPERIMENTAL PROCEDURE

The experiments were performed at the VICKSI accelerator of the Hahn-Meitner-Institut in Berlin. Neutron emission was studied in the reactions ^{141}Pr + ^{40}Ar at 316 MeV ^{40}Ar bombarding energy and ^{175}Lu + ^{12}C at 192 MeV ^{12}C energy leading to the composite systems ^{181}Ir and ^{187}Ir similar to ^{185}Ir in the reaction ^{165}Ho + ^{20}Ne at 220 MeV ^{20}Ne bombarding energy which was investigated previously.[3]

TABLE I. Heavy-ion detector positions in the neutron time-of-flight experiments. For definitions of θ_{lab}, Φ_{lab} see the text, l is the distance from target to heavy-ion detector.

Pr + Ar			Lu + C		
θ_{lab} (deg)	Φ_{lab} (deg)	l (cm)	θ_{lab} (deg)	Φ_{lab} (deg)	l (cm)
−15.0	−9.5	41.2	−15.0	−8.6	15.7
15.0	−8.7	41.4	15.0	−8.6	16.3
−55.0	−9.3	41.6	−40.0	−8.6	15.7
0.0	−33.5	36.6	40.0	−8.6	16.3
			−73.0	−14.7	15.6
			−140.0	−14.7	15.6
			0.0	−53.9	25.8

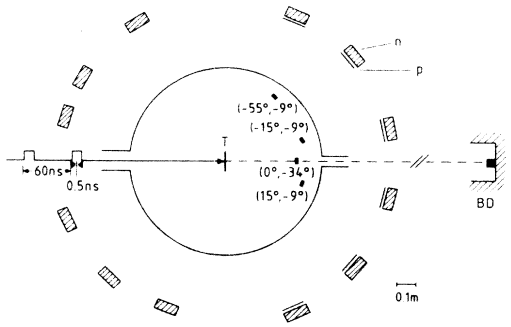

FIG. 1. Schematic diagram of the experimental setup for the time-of-flight experiment. The scintillator paddles "p" were only used in the measurement of Lu + C.

A. Neutron time-of-flight arrangement

In the center of an evacuated scattering chamber with a diameter of 1 m and a 3 mm thick steel wall self-supporting targets were used with thicknesses of 1 mg/cm^2 Pr or 520 μg/cm^2 Lu. Natural praseodymium is monoisotopic ^{141}Pr, whereas natural lutetium contains 97.4% ^{175}Lu and 2.6% ^{176}Lu. In the discussions and calculations we will, however, neglect the contribution from ^{176}Lu. The beam was dumped 5.4 m downstream from the target in a lead-, iron-, and paraffin-shielded Faraday cup. The setup of the experiment is schematically shown in Fig. 1. The heavy reaction products were identified by measuring their energy and time of flight with solid-state detectors positioned inside the chamber. To investigate out-of-plane neutron emission anisotropies the heavy-ion detectors were placed at different positions out of the plane defined by the beam and the neutron detectors. The detector positions for the different measurements are given in Tables I and II. Here θ represents the projection

TABLE II. Neutron detector positions in the neutron time-of-flight experiments (Φ_n=0°). The distance from the target to the neutron detector is l_n.

Pr + Ar		Lu + C	
$\theta_{n\,lab}$ (deg)	l_n (cm)	$\theta_{n\,lab}$ (deg)	l_n (cm)
−11.0	83.8	−10.0	85.1
−39.5	84.7	−40.0	84.2
−65.0	82.9	−70.0	85.5
−123.5	83.4	−100.0	84.5
−149.5	83.6	−135.0	85.1
−165.0	84.0	−165.0	84.5
13.0	85.4	13.0	85.3
40.0	84.7	40.0	83.6
65.0	87.2	70.0	87.6
111.5	81.8	100.0	82.7
135.0	83.6	130.0	83.3
159.0	85.1	159.0	86.2

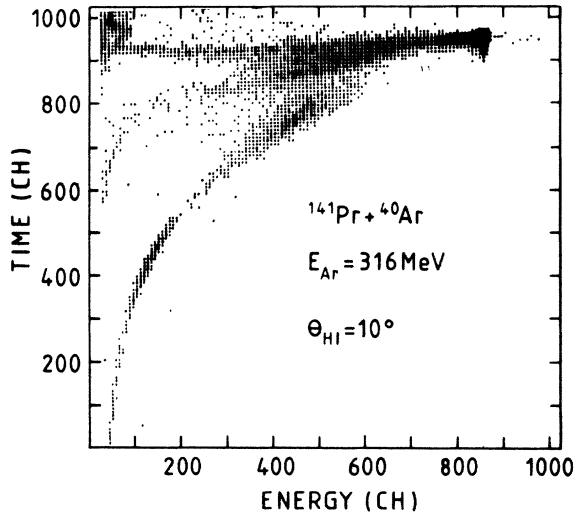

FIG. 2. Two-dimensional raw data plot of the heavy reaction-product flight time versus energy in a 500 μm thick solid-state detector for the reaction Pr + Ar.

of the angle of the solid-state detector with respect to the beam direction onto the plane defined by the beam and the neutron detectors, and Φ is the angle of the detector with respect to this plane. Hence $\theta_{lab}=0°$, $\Phi_{lab}=-53.9°$ in Table I corresponds, e.g., to a geometry, where the plane defined by the detected fission fragment and the beam is perpendicular to the plane defined by the neutron detectors and the fission fragment is detected at 53.9° with respect to the beam below the neutron detector plane.

The time of flight of the heavy reaction products was measured relative to the rf of the cyclotron with a time separation between two bunches of about 60 ns. The separation of fission fragments from other reaction products was done according to their masses and velocities determined by the energy and the flight time as shown in Fig. 2.

Neutrons in coincidence with heavy reaction products were detected with twelve 5 cm thick NE213 liquid scintillators having a diameter of 12.7 cm. All neutron detectors were positioned around the scattering chamber at 12 different angles. Neutrons were detected by measuring the proton recoil energy inside the scintillator and the time of flight relative to the solid-state detector signals. To avoid the detection of low energetic γ rays each neutron detector had a 2 mm thick lead shielding. In order to distinguish neutrons from delayed γ rays at higher energies, γ-n pulse-shape discrimination was employed. Measured time-of-flight spectra for neutrons and γ rays in coincidence with fusion-fission events are shown in Fig. 3. The hardware neutron-detection thresholds were set between 0.3 and 0.4 MeV neutron energy. It is shown in Fig. 3 that without γ-n discrimination delayed γ rays from other reactions and (n,γ) processes of the surrounding material would contaminate the neutron time-of-flight (TOF) distribution. Gammas not rejected (small peak at 22 ns) were separated off line from the TOF spectrum.

The neutron detection efficiencies were calculated as a function of neutron energies and hardware thresholds with a Monte Carlo code from Cecil *et al.*[18] for neutron energies up to 300 MeV. The scintillator light output was calibrated using Compton-edge energies of various radioactive γ-ray sources. Highly energetic charged particles, notably protons with energies larger than 35 MeV may penetrate the 3 mm thick steel wall of the scattering chamber and the scintillator shielding. In order to reject these particles 2 mm thick 15.5 cm times 15.5 cm NE104 plastic scintillator paddles (p in Fig. 1) were placed in front of the forward neutron detectors for the measurement of the reaction Lu + C where highly energetic preequilibrium particles are expected.[3] These paddles were set off line in anticoincidence to the neutron detectors.

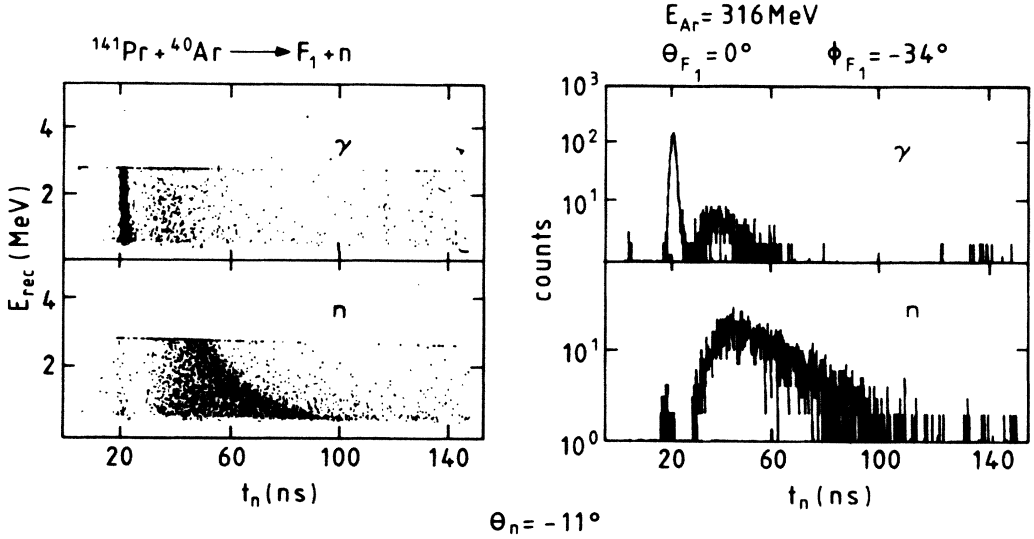

FIG. 3. Two-dimensional plots of the proton recoil energy inside the NE213 scintillator for neutrons and γ rays versus flight time and the respective projections onto the time-of-flight axis for the reaction Pr + Ar.

B. The 4π-scintillator tank

The above-described setup yields information on neutron energy and angular correlations between heavy ions and neutrons which can be used to determine nuclear temperatures and to separate between different neutron sources. The total neutron multiplicities must be extracted indirectly by calculations using the measured parameters because only 2% of the 4π neutron emission is measured with the time-of-flight arrangement. To check the thus deduced total neutron multiplicities experimentally, both reactions were also investigated in a 4π neutron detector[19] which allows the measurement of neutron multiplicities with high efficiency of $\approx 85\%$ for a single neutron. This detector consists of a spherical tank of two halves with a diameter of 1 m which is filled with 500 l NE323 scintillator liquid. A schematic setup is shown in Fig. 4. The beam tube is crossing the center of the tank where a 540 $\mu g/cm^2$ Pr or a 560 $\mu g/cm^2$ Lu target was positioned. The emitted neutrons were detected inside the tank by (n,γ) capture processes in Gd nuclei (Gd is added to the scintillator liquid by 0.5% by weight). The capture γ rays result in light flashes inside the scintillator tank, which are counted. A detailed description of the 4π detector and the neutron detection process is given in Ref. 19. The heavy reaction products were identified by measuring their energy and time of flight with solid-state detectors positioned around the target at different angles.

III. DATA ANALYSIS AND RESULTS

A. Fission-fragment angular distributions

A detailed analysis of the neutron emission in coincidence with fusion-fission events and evaporation residues requires the knowledge of reaction parameters like fusion cross sections and transferred angular momenta. To obtain these parameters we analyzed the measured fission fragment and evaporation-residue angular distributions. The results are compared with those obtained from the reaction Ho + Ne at $E_{lab}=220$ MeV (Ref. 20). The experimental fission fragment angular distributions for both systems (Pr + Ar and Lu + C) are shown in Fig. 5 together with model calculations explained below. The observed anisotropy $W(10°)/W(90°)$ for all three reactions are the same as can be seen from Table III. Obviously there is no dependence of the anisotropy on the entrance-channel mass asymmetry which is different from the observation of Back *et al.*[21]

The fusion cross section σ_{fus} is obtained by the sum of the integrated differential cross sections for evaporation residues σ_{ER} and fission fragments σ_{fiss} and is listed in Table III. The angular-momentum intervals contributing to evaporation-residue formation and fission are deduced from the corresponding cross sections applying the sharp cutoff model. The orbital angular momentum windows contributing to fission (l_{ER}, l_{crit}) are given in Table III.

In the case of a well-defined saddle point, the shape of the fissioning nucleus at that configuration can be determined from the anisotropy of the fission fragment angular distribution applying the transition state model[20,22] (TSM). In this semiclassical model the fission fragment angular distribution is completely determined by the

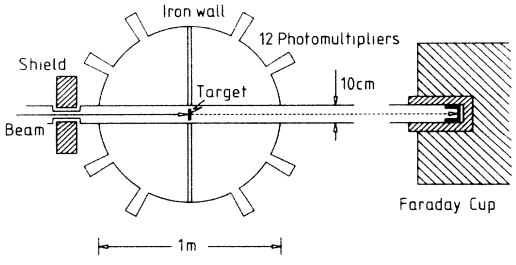

FIG. 4. Schematic setup of the 4π scintillator tank used for total neutron multiplicity measurements.

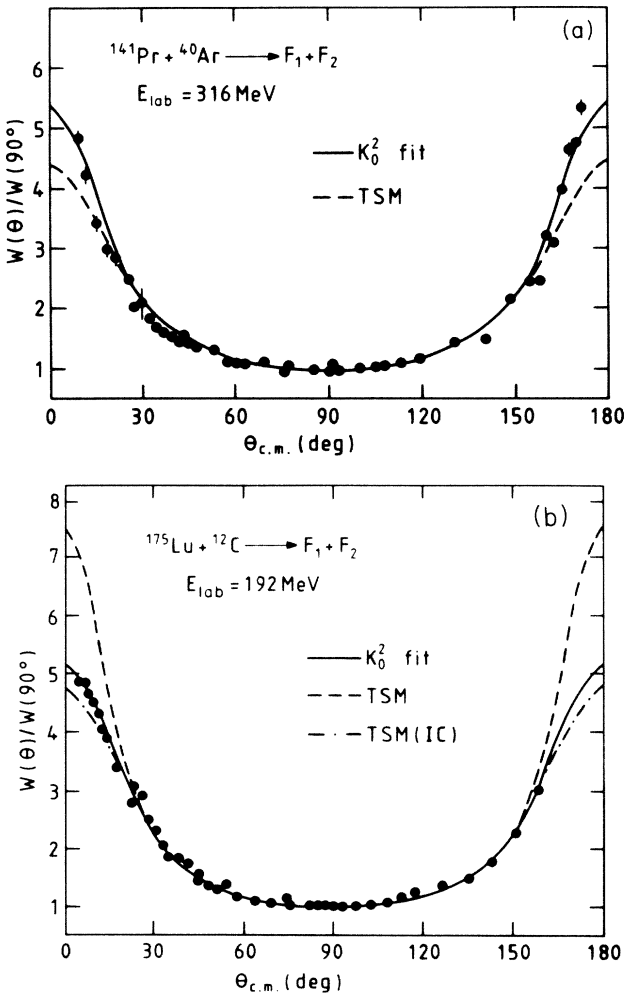

FIG. 5. (a) Fission-fragment angular distribution for the reaction Pr + Ar and comparison with TSM calculations (see the text). The best fit K_0^2 calculation is done according to Eq. (3) for a spin independent K_0^2. (b) Fission fragment angular distribution for the reaction Lu + C and comparison with TSM calculations under the assumption of complete (TSM) and incomplete fusion [TSM(IC)]. The best fit K_0^2 is again considered to be independent of the spin.

TABLE III. Results from evaporation-residue and fission-fragment angular-distribution measurements.

Reaction	σ_{ER} (mb)	σ_{fiss} (mb)	σ_{fus} (mb)	l_{ER} ($\hbar$)	l_{crit} ($\hbar$)	K_0^2	$\frac{W(10°)}{W(90°)}$
$^{141}Pr + {}^{40}Ar$	220±50	811±30	1031±130	50±6	109±7	363±64	4.6±0.3
$^{175}Lu + {}^{12}C$	1162±260	663±70	1825±340	59±9	74±7	258±52	4.5±0.4
$^{175}Lu + {}^{10}B$	1162±260	663±70	1825±340	49±6	62±6	258±52	4.5±0.4
$^{165}Ho + {}^{20}Ne$[a]	620±60	1070±110	1690±170	57±3	94±5	285±15	4.8±0.1

[a]Reference 20.

quantum numbers I, K, and M. Here K is the projection of the total spin I onto the nuclear symmetry axis which is identical with the fission axis in this model, and M is the projection of I onto a space fixed axis. The K distribution function is taken as $\exp\{-K^2/K_0(I,K)\}$ with

$$K_0^2(I,K)=\frac{J_{sph}}{\hbar^2}\frac{T(I,K)}{J_{sph}/J_{eff}(I,K)}\ , \tag{1}$$

where

$$T(I,K)=\{[E^*-B_F(I,K)-E_{rot}(I,K)]/(A/8)\}^{1/2}$$

is the nuclear temperature at the saddle point (SP) and J_{sph} is the rigid-body moment of inertia of a sphere. The fission barrier B_F and the effective moment of inertia J_{eff} depends on the orientation of the fission axis with respect to the spin axis[23] and can be written as

$$B_F(I,K)\sim B_F(I,0)+E_{rot}^{SP}(I,K)-E_{rot}^{CN}(I,K)\ ,$$
$$J_{eff}(I,K)=J_{||}(I,K)J_{\perp}(I,K)/[J_{\perp}(I,K)-J_{||}(I,K)]\ . \tag{2}$$

Here $B_F(I,0)$, E_{rot}^{SP}, E_{rot}^{CN}, $J_{||}(I,K)$, and $J_{\perp}(I,K)$ are, respectively, the rotating liquid drop model (RLDM) (Ref. 24) fission barrier at $K=0$, the rotation energy at the saddle point, the ground-state configuration, and the moment of inertia of the rotating liquid drop parallel and perpendicular to the nuclear symmetry axis at spin $R=\sqrt{I^2-K^2}$. The fission fragment angular distribution is given by[22]

$$W(\theta)\sim\sum_I(2I+1)T_I\frac{\sum_{K=-I}^{I}(I+0.5)\,|\,D^I_{M=0,K}(\theta)\,|^2\exp\left[-\frac{K^2}{2K_0^2(I,K)}\right]}{\sum_{K=-I}^{I}\exp\left[-\frac{K^2}{2K_0^2(I,K)}\right]}\ , \tag{3}$$

where T_I is the transmission coefficient and the $D^I_{M,K}$ are the normalized rigid-rotor functions.

In Fig. 5 the experimental fission-fragment angular distributions are compared with predictions of the TSM. At high spin values where the fission barrier vanishes, the effective moment of inertia cannot be computed by the RLDM. In this case we arbitrarily assumed $J_{sph}/J_{eff}=0$. For the fusion-fission reaction of Lu + C the agreement between measured and calculated anisotropies is improved when the effects of incomplete fusion are taken into account. Computations for incomplete fusion assuming multiple α breakup of carbon are also shown in Fig. 5(b). The respective maximum orbital angular momentum for fusion of α particles, ^{8}Be or ^{12}C, respectively, is assumed to be[25] $l_{max}=\frac{7}{5}N_p$, where N_p is the number of l waves with a pocket in the interaction potential of the fusing system and the factor $\frac{7}{5}$ accounts for the loss of angular momentum due to friction. An approximate determination of the incomplete fusion by the experimental evaporation residue velocity spectrum is given in Sec. IV. In addition, the experimental angular distributions were fitted with a spin-independent value of K_0^2 in Eq. (3). The best-fit values of K_0^2 are given in Table III and the corresponding calculated angular distributions are shown in Figs. 5(a) and (b). With the assumption that the shape of the fissioning nucleus is a spheroid with ratio $d=c/a$ of the principal half axis c and a, it is possible to estimate the shape of the fissioning nucleus which determines the K distribution. The relation between d and K_0^2 is given by

$$\frac{d^{2/3}+d^{-4/3}}{d^{4/3}-d^{-2/3}}=\frac{\hbar^2K_0^2}{TJ_{sph}}\ . \tag{4}$$

Using a radius parameter of $r_0=1.2249$ fm and the experimentally determined nuclear temperatures T (see Sec. III B), one obtains $d=1.5$, $d=1.7$, and $d=1.9$ for the reactions Pr + Ar, Ho + Ne, and Lu + C, respectively. The deduced deformation increases with decreasing mean spin $\langle I\rangle$, which indicates that the K distribution is frozen in at shapes that are less compact for smaller $\langle I\rangle$. The deformation parameters d are used in Sec. IV A to calculate the prescission neutron multiplicities.

B. Neutron evaporation in coincidence with fission products

Neutron emission in coincidence with fusion-fission events and evaporation residues was measured for the above-discussed two systems Pr + Ar at 316 MeV and Lu + C at 192 MeV bombarding energy.

In the reaction Pr + Ar central heavy-ion collisions

lead to the composite system ^{181}Ir with a fissility parameter of $x=0.67$. It is assumed that this system fissions for $l_{ER} < l < l_{B_F=0} \approx 80\hbar$ via a saddle point and for $l_{B_F=0} < l < l_{crit} = 109\hbar$ via a symmetric[9,26] fragmentation process, sometimes also called "fast fission." Both the highly excited composite system prior to scission as well as the two fission fragments deexcite mainly by neutron evaporation. Thus we have three neutron evaporation sources, if we neglect evaporation during the acceleration phase of the fission fragments, which will be discussed in Sec. IV: (i) the composite system prior to scission, (ii) the detected fully accelerated fission fragment, and (iii) the correlated fully accelerated fission fragment.

All neutron energy spectra were measured in coincidence with fission fragments detected at four fixed trigger angles (see Table I). In order to parametrize the experimental spectra we applied a three-source least-squares-fit analysis to the data assuming complete fusion, symmetric fission, and isotropic neutron emission in the rest frame of each source. The spectral shape of the fit function in the laboratory frame is given by a Watt distribution:[3]

$$\frac{d^2M_n}{dE_n d\Omega_n} = \sum_{i=1}^{3} \frac{M_i \sqrt{E_n}}{2(\pi T_i)^{3/2}} \times \exp\left[\frac{E_n - 2\sqrt{\epsilon_i \cdot E_n}\cos\Psi_i + \epsilon_i}{T_i}\right] . \quad (5)$$

Among all variables used in Eq. (5) we take, as known, the energy per nucleon ϵ_i of the source and the neutron emission angle Ψ_i relative to the source i. The nuclear temperatures T_i and the neutron multiplicities M_i were taken as free parameters, determined by the least-squares fit of the measured neutron spectra at all 12 different neutron detection angles. For the two symmetric fission fragments we assumed the same temperature and neutron multiplicity after we found that these parameters were equal if they were searched for independently. One example for experimental neutron energy spectra measured in coincidence with fission fragments is shown in Fig. 6 together with the results of the fit for all three neutron emission sources. It was possible to fit the data under the assumption of isotropic emission in the rest frame even for the case where the neutrons were detected in a plane perpendicular to the reaction plane defined by the fission fragments as shown in Figs. 6 and 7(a). As expected for evaporated neutrons, no out-of-plane anisotropy is observed. We will return to this point in more detail in this section when discussing the preequilibrium emission (PE) from the system Lu + C. The neutron yield integrated over neutron energies between 2 and 10 MeV together with the obtained best fits are shown as a function of the neutron detection angle in Fig. 7(a) for all measured fragment trigger angles. The corresponding reaction geometries are shown in Fig. 7(b). All results of the fit procedure are given in Table IV. As can be seen from Fig. 7(a) it is possible to reproduce quite well different neutron angular correlations at different trigger angles by

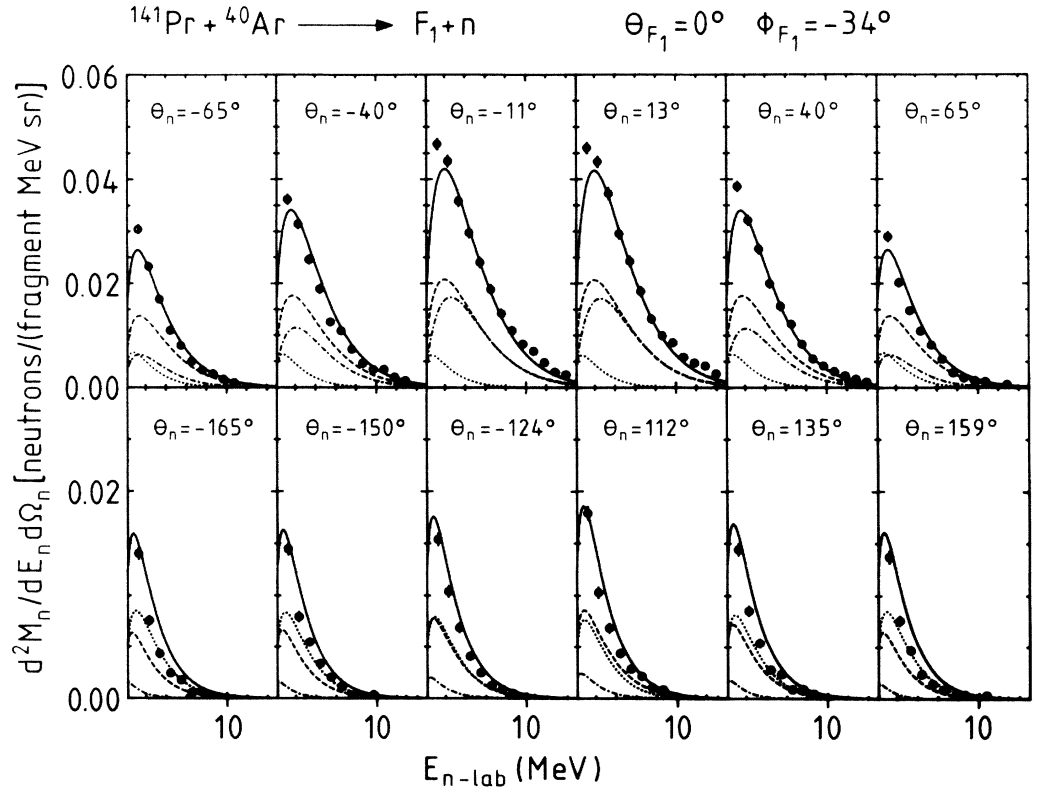

FIG. 6. One example for experimental double differential neutron multiplicities as a function of the neutron energy in coincidence with fusion-fission events in the reaction Pr + Ar. The solid lines represent the sum of the evaporative components of the composite system prior to scission (— — —), the detected (—·—·—·), and the correlated (· · · ·) fission fragment.

TABLE IV. Mean parameters obtained by the least-squares fit of neutron energy spectra in coincidence with fusion-fission events for all three reactions. The affix "presc" and "post" stands for prescission and postscission neutrons.

		Evaporation				Preequilibrium (PE)			
	Reaction	M_n^{presc} (neutrons)	M_n^{post} (neutrons)	T^{presc} (MeV)	T^{post} (MeV)	M_n^{PE} (neutrons)	T^{PE} (MeV)	ϵ^{PE} (MeV/nucleon)	a_n^{PE}
	Pr + Ar	3.6±0.6	4.4±0.4	2.2±0.3	1.7±0.3				
FF	Ho + Ne[a]	5.6±0.5	3.7±0.7	2.6±0.3	1.5±0.3	0.4±0.1	5.9±0.3	2.6±0.2	0.0
	Lu + C	5.2±0.6	3.0±0.4	2.3±0.1	1.3±0.2	0.4±0.1	7.3±0.1	2.2±0.8	2.2±0.6
		(6.3±0.8)[b]	(3.6±0.5)[b]			(0.5±0.2)[b]			
ER	Lu + C	6.7±0.3		2.1±0.1		0.5±0.1	7.5±0.6	3.1±0.4	0.0
		(8.5±0.4)[b]				(0.6±0.2)[b]			

[a]Reference 3.
[b]Renormalized values according to the measurement of total neutron multiplicity (cf. Sec. III D).

using one set of fit parameters although the correlations are completely different due to the different kinematical situations. This can be taken as an additional proof that the employed parametrization is indeed correct. However, there are small deviations between the calculation and the data for some neutron detection angles as shown in Fig. 6 which can also be seen in Fig. 7(a). A more detailed consideration of the deviations gave no evidence for the assumption that these differences are due to shadowing of neutrons by fission fragments or to neutron emission from the elongated neck at the moment of rupture, which could give an additional yield of neutrons not taken into account by the multiple source fit.

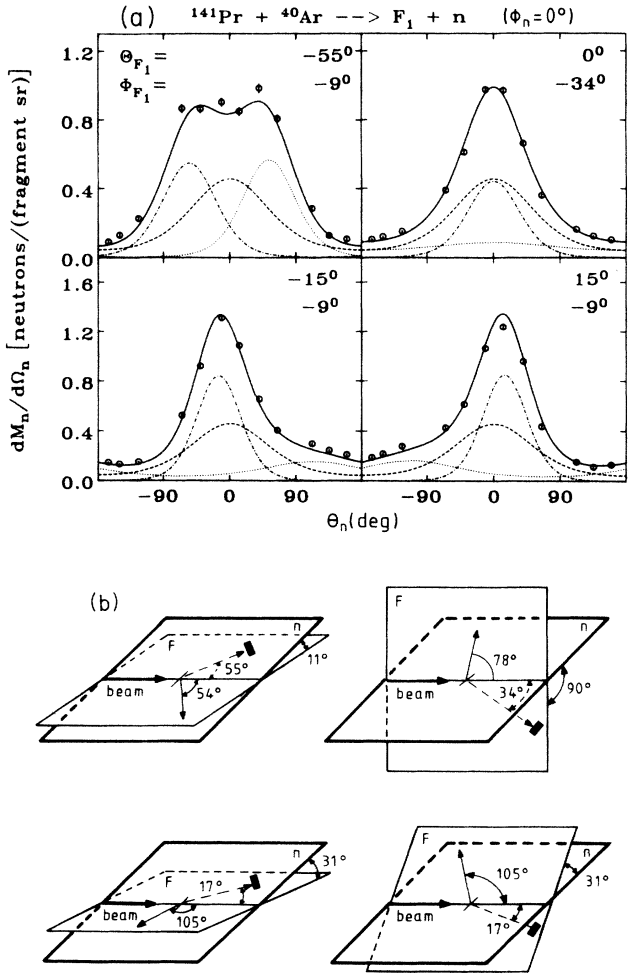

FIG. 7. (a) All measured angular correlations for neutrons detected in coincidence with fission-fragments detected at different fixed trigger angles θ_{F_1}, Φ_{F_1} in the reaction Pr + Ar. The neutron energies are integrated between 2 and 10 MeV. The solid curves denote the sum of the contributions from the three evaporation sources (see Fig. 6). (b) The respective reaction geometries. The reaction plane F is defined by the heavy-ion detector (direction of the fission fragment) and the beam axis. The neutron detection plane n is defined by the various neutron detectors and the beam axis. The polar angle ϑ (angle between the beam direction and the heavy-ion detector) and the azimuthal angle φ (angle between the two planes n and F) are shown.

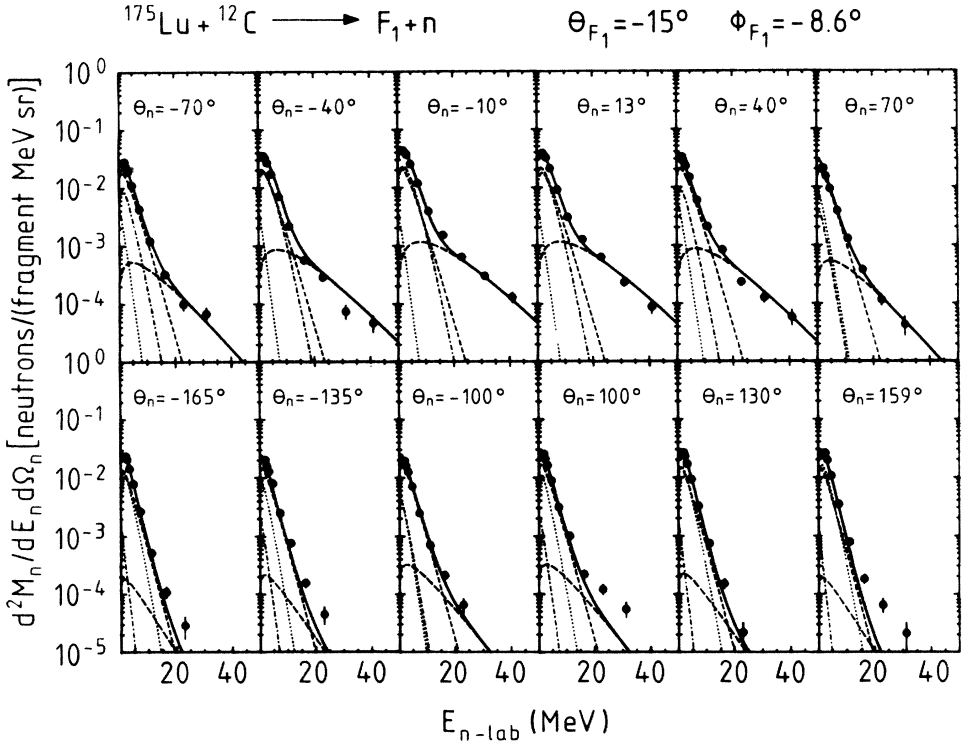

FIG. 8. One example of the measured neutron energy spectra in coincidence with fusion-fission events in the reaction Lu + C. In addition to the three evaporative components (see Fig. 6) a highly energetic preequilibrium neutron component (— — —) is present.

We now turn to the neutron emission in coincidence with fusion-fission events for the reaction Lu + C. As calculated from the measured σ_{fus} under the assumption of complete fusion, the critical angular momentum leading to fusion is $l_{\text{crit}} = 74\hbar < I_{B_F=0} \approx 80\hbar$ so that we can consider this system as a "normal fission system." Because of the high projectile energy of 16 MeV/nucleon we expect preequilibrium neutron emission.[3] To take this into account, we parametrized the experimental neutron energy spectra by adding a fourth source to the above-described least-squares-fit analysis of the data. The spectral shape is again given by Eq. (5) with ϵ_{PE}, M_{PE}, and T_{PE} as additional fit parameters. One example for experimental neutron energy spectra measured in coincidence with fission fragments is shown in Fig. 8 together with the fit results for all neutron emission sources. The results of the fit procedure are given and compared with those obtained from the reactions Pr + Ar and Ho + He (Ref. 3) in Table IV. The energy-integrated angular correlations for all measured trigger angles and the obtained best fits are shown in Fig. 9. All three systems considered in Table IV show relatively large prescission neutron multiplicities. It is interesting to note that for the two very asymmetric systems Lu + C and Ho + Ne about 60% of the evaporated neutrons are emitted prior to scission, whereas for the system Pr + Ar the same quantity is only 45%. The small value for Pr + Ar is probably due to the larger angular momentum brought into the system. A detailed interpretation of the large neutron multiplicities prior to scission and its correlation to the lifetimes of these systems prior to scission is given in Sec. IV.

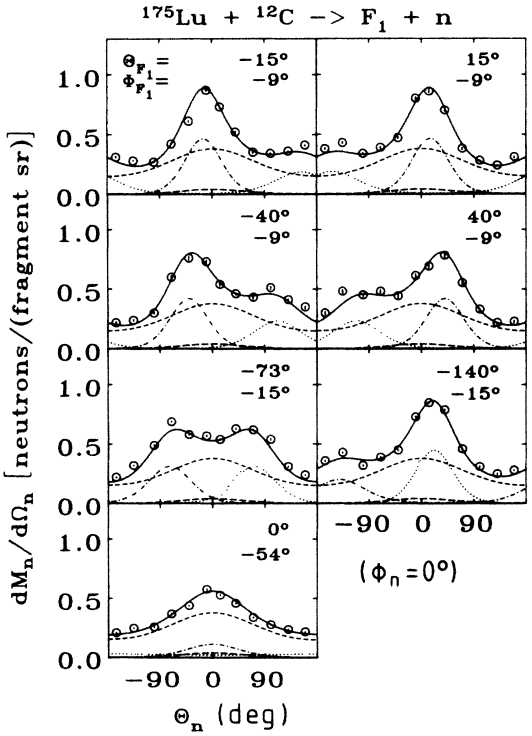

FIG. 9. All measured angular correlations for neutrons detected in coincidence with fission fragments at different fixed trigger angles θ_{F_1}, Φ_{F_1} in the reaction Lu + C. The neutron energies are integrated between 2 and 10 MeV. The solid curves denote the sum of the contribution from the three evaporative and one preequilibrium source.

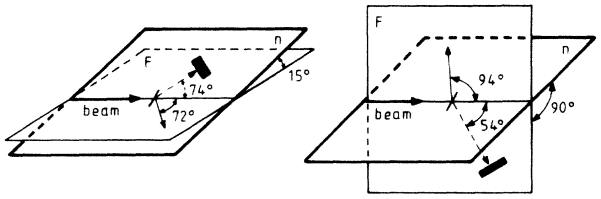

FIG. 10. Two different reaction geometries for an "in-plane measurement" where the neutrons are detected in a plane n rotated only 15° against the fission plane F and for an "out-of-plane measurement" where F and n are perpendicular to each other.

C. Preequilibrium neutron emission

We now want to consider the preequilibrium neutron emission in the reaction Lu + C. The fit results given in Table IV are obtained by applying the four-source fit procedure to the experimental neutron energy spectra measured in coincidence with fission fragments and evaporation residues. In Fig. 10 two different reaction geometries are shown schematically. In this figure the polar angle ϑ of the solid state detector, with respect to the beam direction and the azimuthal angle φ between the fission plane F and the neutron detector plane n, is shown. It was not possible to achieve a reasonable good fit of the high energy component in the neutron spectra in coincidence with fission fragments, under the assumption of isotropic emission of this component in the rest frame for the case in which the planes F and n were perpendicular to each other.

Under the assumption of $K=0$ and $M=0$ (cf. Sec. III A), the spin is perpendicular to the beam and to the fission axis. Consequently, the spin vector lies in the neutron detector plane n only for geometries in which the two planes F and n are perpendicular to each other. Since for this geometry we observed deviations between the data and the best fit calculations, as shown in Fig. 11, under the assumption of isotropic neutron emission in the rest frame of the preequilibrium source, we included in the fit function the following anisotropic[27] neutron emission in the rest frame of this source:

$$\frac{d^2M_n}{dE_n d\Omega_n}=\frac{d^2M_n^0}{dE_n d\Omega_n}\exp(-a_n^{PE}\cos^2\Delta)\ . \tag{6}$$

Here Δ is the angle between the spin vector of the composite system and the direction of the emitted neutron ($d^2M_n^0/dE_n d\Omega_n$) is the expression of the double differential neutron multiplicity in the rest frame of the source for isotropic neutron emission, and a_n^{PE} is the anisotropy parameter. Renormalization and transformation into the laboratory frame leads to the fit function:

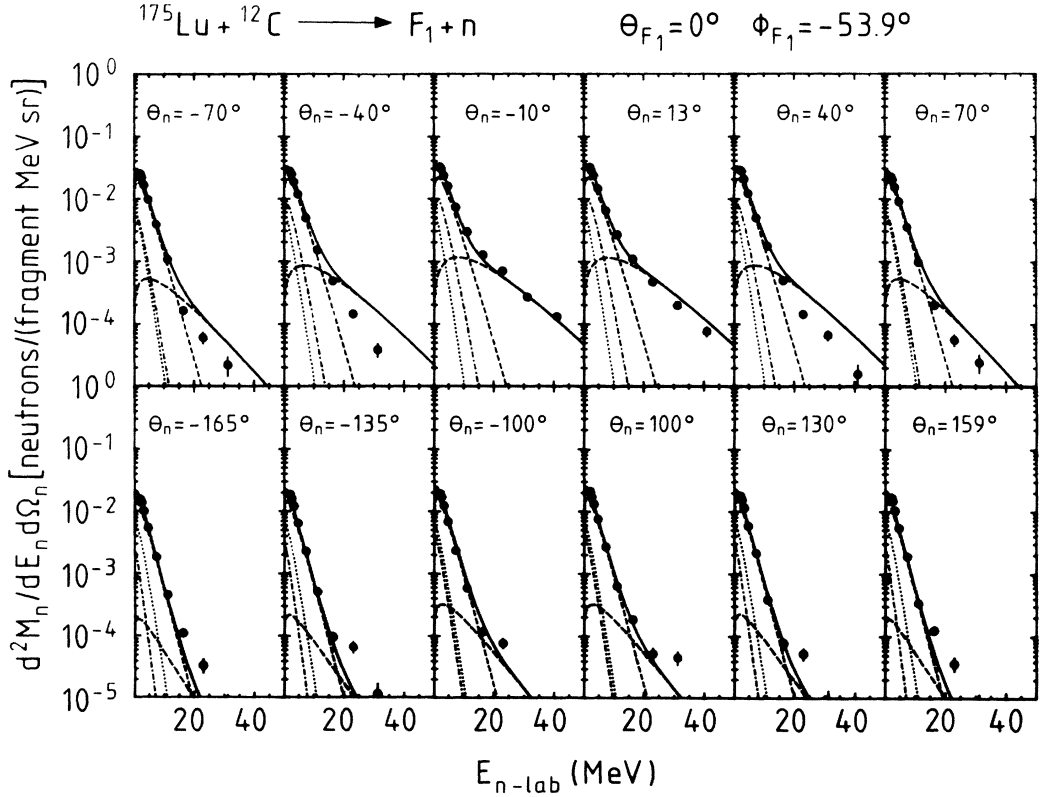

FIG. 11. Experimental neutron energy spectra measured in coincidence with fission fragments detected in a plane F perpendicular to the neutron detector plane n in the reaction Lu + C. The fit calculation for the highly energetic preequilibrium neutron emission was performed assuming isotropic emission in the rest frame of the source.

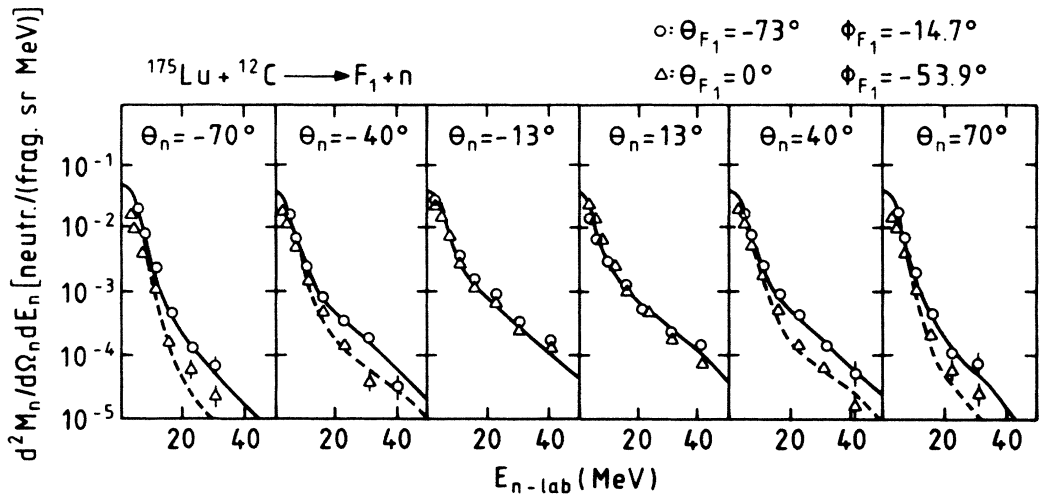

FIG. 12. Comparison between experimental neutron energy spectra measured "in plane" and "out of plane" in coincidence with fission fragments according to geometries shown in Fig. 10 in the reaction Lu + C. The calculation (solid line) for the "in-plane measurement" (○○○) was done assuming isotopic emission in the rest frame of each source. The calculation (dashed line) for the "out-of-plane measurement" (△△△) was obtained by assuming anisotropic preequilibrium neutron emission according to Eq. (7).

$$\frac{d^2M_n}{dE_n d\Omega_n} = \frac{M_n\sqrt{E_n}}{2(\pi T)^{3/2}N}\exp\left[-\frac{E_n - 2\sqrt{\epsilon \cdot E_n}\cos\Psi + \epsilon}{T}\right] \times \exp\left[-\frac{a_n^{PE} E_n \sin^2\Psi}{E_n + \epsilon - 2\sqrt{E_n \epsilon}\cos\Psi}\right] \quad (7)$$

with the renormalization factor

$$N = \int_0^{\pi} \exp(-a_n^{PE}\cos^2\Psi)\sin\Psi\, d\Psi \, .$$

The fit results for the preequilibrium neutron emission using Eq. (7) are given in Table IV. The fitted asymmetry parameter of $a_n^{PE} = 2.2$ describes a very strong anisotropy

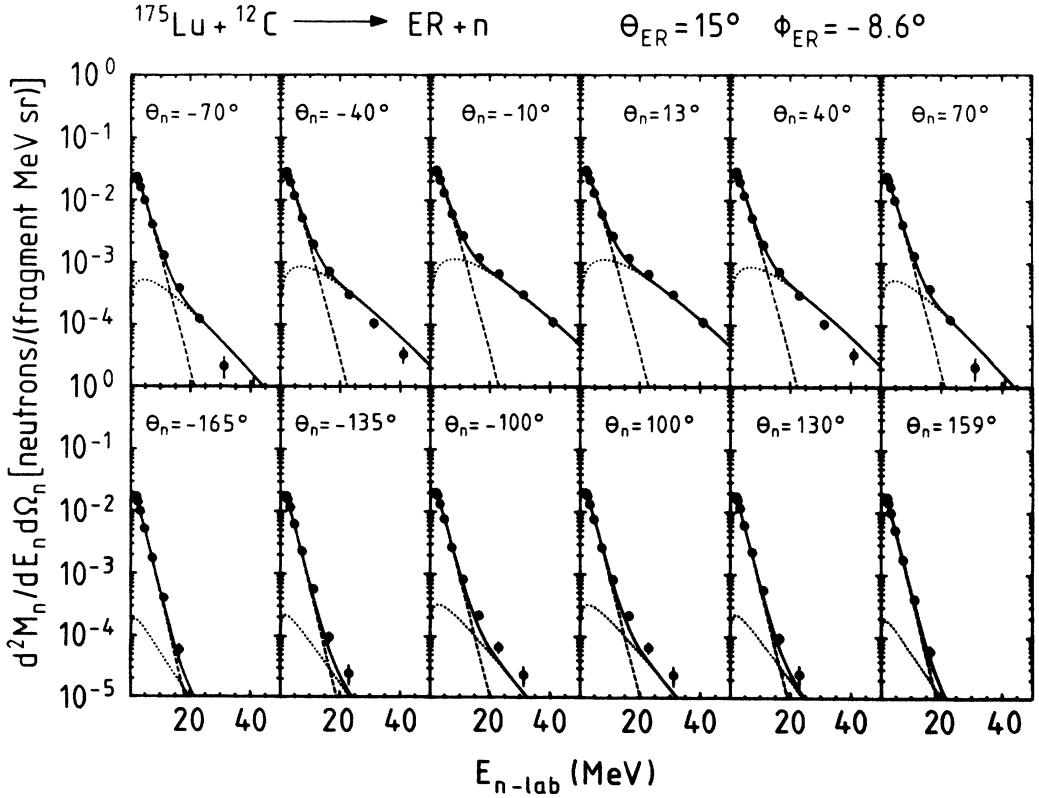

FIG. 13. Experimental neutron energy spectra measured in coincidence with evaporation residues in the reaction Lu + C. The fit calculation for the preequilibrium neutron emission was done under the assumption of isotropic emission in the rest frame of the source according to Eq. (5).

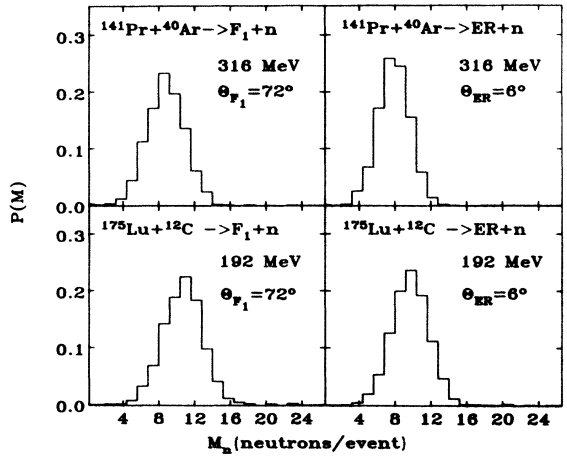

FIG. 14. Typical total neutron multiplicity distributions measured with the 4π scintillator tank in coincidence with fission fragments and evaporation residues (ER) for the reactions Pr + Ar and Lu + C.

of the preequilibrium emission with respect to the spin direction of the composite system, whereas for the evaporation of low energetic neutrons from the fully equilibrated system no anisotropy was observed.

The effect of the anisotropic preequilibrium neutron emission is evident in Fig. 12 where the experimental neutron energy spectra in coincidence with fission fragments are compared for the two reaction geometries shown in Fig. 10. In Fig. 12 the observed out-of-plane emission is denoted by triangles, and the results of the in-plane measurements are denoted by circles. The lines are fit calculations using Eqs. (5) and (7) denoted by the solid and the dashed curve, respectively. The reduction of the emission out of plane is clearly visible. For the preequilibrium emission of charged particles a similar anisotropy was reported by Tsang *et al.*[28]

The observed enhancement of preequilibrium neutron emission in the reaction plane might be understood in a model[25,29] in which complete fusion is limited by the angular momentum. The excess angular momentum brought into the system is then carried away by light particles with approximate beam velocity and preferential emission perpendicular to the spin. Also the Harvey-Homeyer model[30] of direct massive transfer implies such a behavior.

For the system Lu + C we have also investigated the neutron emission in coincidence with evaporation residues. The heavy recoils were measured at about 17° in the laboratory frame. At this relative large angle the heavy recoils are not necessarily evaporation residues, but can be contaminated with targetlike recoils due to massive transfer reactions. Therefore it was necessary to gate the neutrons only with the high velocity part of the heavy recoils. We have considered all heavy recoil (HR) products having a velocity $V_{HR} \geq 0.25$ cm/ns as evaporation residues, but there might still be a small contamination by targetlike recoils even for higher velocities. The mean V_{ER} is 0.3 cm/ns whereas the velocity corresponding to full momentum transfer is $V_{ER} = 0.36$ cm/ns. The experimental values, however, are uncertain to about 10% because of the plasma delay[31] associated with the detection of heavy fragments.

In order to correct for the asymmetry[32] introduced into the neutron spectrum and angular distribution by the recoil of the detected neutron on the ER, we averaged the neutron spectra measured in coincidence with evaporation residues at 17° over symmetric neutron angles left and right to the beam axis. The averaged experimental spectra were parametrized by applying a two-source least-squares-fit analysis assuming one evaporation and one preequilibrium source both emitting isotropically in their rest frames. The experimental data together with the best fits are shown in Fig. 13 and the parameters are given in Table IV.

D. Total neutron multiplicities

To check the neutron multiplicities in coincidence with fusion-fission events and evaporation residues obtained by the applied fit procedure to the neutron energy spectra, the total multiplicities were also measured directly with the 4π-neutron detector described in Sec. II. For both reactions Pr + Ar and Lu + C the neutron multiplicities were measured in coincidence with fusion-fission events at different trigger angles and evaporation residues at $\theta_{ER} = 2.2°$ and 6°. The experimental multiplicity spectra were corrected for the background and the efficiency of the detector determined by a ^{252}Cf calibration measurement. Typical corrected multiplicity spectra are shown in Fig. 14 and the results are compared with those obtained by the neutron time-of-flight measurement and the applied fit procedure in Table V. There is good agreement for the reaction Pr + Ar but a difference of 19%, corresponding to 1.6 standard deviations for the reaction

TABLE V. Total neutron multiplicities measured in coincidence with evaporation residues and fusion-fission events with a 4π scintillator tank and comparison with those obtained by the least-squares fit procedure.

Reaction	Coincident fragment	4π tank M_n^{tot} (neutrons)	TOF measurement M_n^{tot} (neutrons)
Pr + Ar	ER	7.86±0.09	
Pr + Ar	FF	8.45±0.04	8.0±1.0
Lu + C	ER	9.14±0.07	7.2±0.4
Lu + C	FF	10.36±0.04	8.6±1.1

Lu + C. Assuming that the difference is originating from a systematic error made in the fit procedure applied to the neutron energy spectra as described in Sec. III B, one has to renormalize the neutron multiplicities of each source by the factor 10.4/8.6 leading to $M_n^{presc}=6.3$ for the prescission neutron multiplicity. The difference between the results of both measurements for the neutrons in coincidence with evaporation residues can be due to the contamination of evaporation residues with targetlike recoils at the detection angle of $\approx 17°$ at the time-of-flight measurement, whereas for $\theta_{ER}=2.2°$ and 6° at the total multiplicity measurement the contribution of heavy recoils with a smaller neutron multiplicity can be excluded.

As described in Sec. II the neutron energy thresholds used in the neutron time-of-flight experiment were 0.3–0.4 MeV. Due to possible uncertainties or instabilities in these thresholds the efficiencies of the neutron detector can vary drastically for energies close to the threshold. That is why all least-squares fits were performed for neutron energies larger than 1.6 MeV. Consequently, it is necessary to extrapolate the neutron energy spectra to zero energy in order to obtain absolute neutron multiplicities. This uncertainty could have also caused the above-observed discrepancy between the neutron multiplicities as measured with the time-of-flight arrangement and the 4π neutron tank. In the following discussion we will only use the renormalized value.

As a conclusion of this section we point out that for both measured reactions which lead to composite systems with similar excitation energy $E^* \approx 164$ MeV as the previously measured reaction[3] Ho + Ne at 220 MeV ^{20}Ne bombarding energy a considerable neutron emission occurs before the system fissions even for so-called "fast fission systems"[9,26] like Pr + Ar. Furthermore, a strong anisotropy was observed for the preequilibrium neutron emission with respect to the spin of the composite system formed in the reaction Lu + C, whereas no such anisotropy was observed for evaporative neutrons.

In the next section the results concerning the high prescission neutron multiplicities are discussed by comparing the results with modified statistical model calculations.

IV. DISCUSSION AND COMPARISON WITH MODELS

A. Evaporative neutron emission of the composite systems prior to scission

To obtain information about the fission dynamics of highly excited nuclei the experimental prescission neutron multiplicity is compared in the following with statistical model calculations (code JULIAN) (Ref. 33) performed for

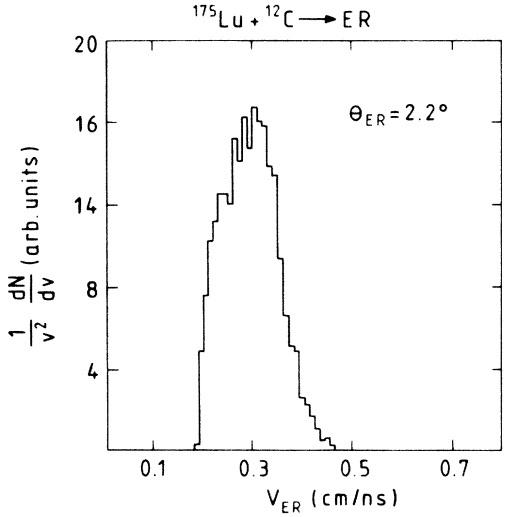

FIG. 15. Galilean invariant velocity distribution of evaporation residues for the reaction Lu + C.

different steps of the fission process.

The code calculates nuclear evaporation of neutrons, protons, and α particles in competition to fission taking into account angular momenta and using optical-model transmission coefficients and Fermi-gas level densities. The following parameters were used in the calculations. The level density parameter of the compound nucleus a_n (Refs. 34 and 35) and of the transition state nucleus a_f were set to $a_f=a_n=A/10$. The RLDM fission barrier[24] was lowered by the factor 0.8 (Ref. 36) and set to zero for angular momenta $I \geq I_{B_F=0}$. Transmission coefficients of the evaporated particles were computed from optical model potentials of Wilmore and Hodgson[37] for neutrons, of Perey[38] for protons, and of Huizenga and Igo[39] for alpha particles. We further assumed complete fusion for the systems Pr + Ar and Ho + Ne. For the reaction Lu + C an approximation for the amount of incomplete fusion was made using the velocity spectrum of evaporation residues as measured in the neutron-sphere experiment over a flight path of 70 cm at 2.2°. The Galilean invariant cross section $(1/v^2)d\sigma/dv$ is shown in Fig. 15. The mean value of this distribution is 0.30 cm/ns which corresponds to a linear momentum transfer of 85% and thus complete fusion of ^{10}B and ^{175}Lu on the average at $E_{lab}(^{10}B)=159$ MeV. Fission probabilities $\sigma_{fiss}/\sigma_{fus}$ calculated with these assumptions are in good agreement with the experimental ones and given in Table VI.

This can be taken as an indication that the chosen parameters are correct because there is a strong dependence of the calculated fission probabilities on the input parame-

TABLE VI. Comparison between experimental fission probabilities $(\sigma_{fiss}/\sigma_{fus})^{expt}$ and the calculated ones $(\sigma_{fiss}/\sigma_{fus})^{JULIAN}$ using the statistical model code JULIAN.

System	$(\sigma_{fiss}/\sigma_{fus})^{expt}$	$(\sigma_{fiss}/\sigma_{fus})^{JULIAN}$
^{165}Ho + ^{20}Ne (Ref. 20)	63.3±5%	68.9%
^{141}Pr + ^{40}Ar	78.7±6%	78.9%
^{175}Lu + ^{10}B(^{12}C)	36.3±9%	30.7% (52.9%)

ters a and a_f/a_n. By changing, e.g., a, by about 20% or a_f/a_n by about 3–5 %, the calculated fission probabilities vary by about 15%.

As noted in Refs. 40 and 41 the radius parameter r_0 used to calculate transmission coefficients for evaporated particles can be deduced from the experimental energy spectra. However, within our measured energy range, the neutron spectra are not sensitive enough to determine this parameter. Employing several evaporation calculations, a rather weak dependence of the prefission neutron multiplicity on r_0 has been observed. For instance, by increasing the radius by 20% and decreasing the fission barrier by 50% in order to keep the fission probability $\sigma_{\rm fiss}/\sigma_{\rm fus}$ close to the observed value, one obtains for the reaction Ho + Ne $\sigma_{\rm fiss}/\sigma_{\rm fus}=60\%$, a neutron multiplicity for evaporation residues of $M_{\rm n}^{\rm ER}=6.4$ and a prefission neutron multiplicity of $M_{\rm n}^{\rm prefiss}=1.8$. The quantities $\sigma_{\rm fiss}/\sigma_{\rm fus}$ and $M_{\rm n}^{\rm prefiss}$ are similar to the results obtained by our standard parameters whereas the value of $M_{\rm n}^{\rm ER}$ is lowered by 30% which does not agree with the experimental result.

The mean prefission neutron multiplicities $M_{\rm n}^{\rm prefiss}$ calculated by JULIAN are 1.1, 1.9, and 4.5 for the systems Pr + Ar, Ho + Ne, and Lu + B, respectively. The experimentally deduced prescission neutron multiplicities are 3.6±0.6, 5.6±0.5, and 6.3±0.8, respectively, which are clearly larger. However, the relative discrepancy is decreasing with decreasing critical angular momentum.

There are three possibilities for the emission of the remaining prescission neutrons not predicted by JULIAN as prefission neutrons. The first one is the evaporation of neutrons during the formation phase of the composite system. The underlying assumption is that the relaxation time for the mass asymmetry degree of freedom is longer than that for the excitation energy. Otherwise these neutrons would be preequilibrium neutrons, which are not observed in the reaction Pr + Ar. The formation time depends on the mass asymmetry of the entrance channel[9] and should be larger for the system Pr + Ar (small mass asymmetry) than for the reactions Ho + Ne and Lu + C (larger mass asymmetry). If there would be neutron evaporation during the formation time of the composite system the difference between the measured prescission and calculated prefission neutron multiplicities should increase with decreasing mass asymmetry. This expectation, however, does not agree with the obtained values for these excess neutrons of 1.8±0.2, 3.7±0.3, and 2.5±0.4 for the systems Lu + C, Ho + Ne, and Pr + Ar, respectively. This seems to indicate that there is no considerable neutron evaporation during the formation of the composite system and the excess neutrons must be due to another process.

The second possibility to understand the high experimental prescission neutron multiplicities is the evaporation of neutrons from not fully accelerated fission fragments.[3,5] As long as the velocities of the accelerating fragments are small, neutrons emitted from these fragments will be considered experimentally as prescission neutrons focused kinematically into the same forward direction as the neutrons emitted from the composite system. Model calculations of angular correlations of evaporated neutrons from fission fragments as a function of fragment kinetic energies can show[3] for which kinetic energies during the acceleration phase the neutron angular correlation becomes sufficiently distinguishable from the angular correlation of the composite system. Such calculated angular correlations are shown in Fig. 16 for symmetric trigger angles assuming two spheres with a charge $Z/2=38$ which are accelerated in their mutual Coulomb field and start with zero relative energy at the moment of separation. We find that for kinetic energies between 60 and 80 MeV for the system Pr + Ar and 30 and 60 MeV for the systems Ho + Ne and Lu + C, the neutron angular correlation becomes double peaked and well distinguishable from the angular correlations of the composite system. These kinetic energies correspond to acceleration times of $(1-3)\times10^{-21}$ s. Neutrons emitted from both fission fragments during these times would be considered experimentally as prescission neutrons.

Because of these relatively short acceleration times neutron emission from not fully accelerated fission fragments cannot explain the difference between calculated prefission and experimental prescission neutron multiplicities.

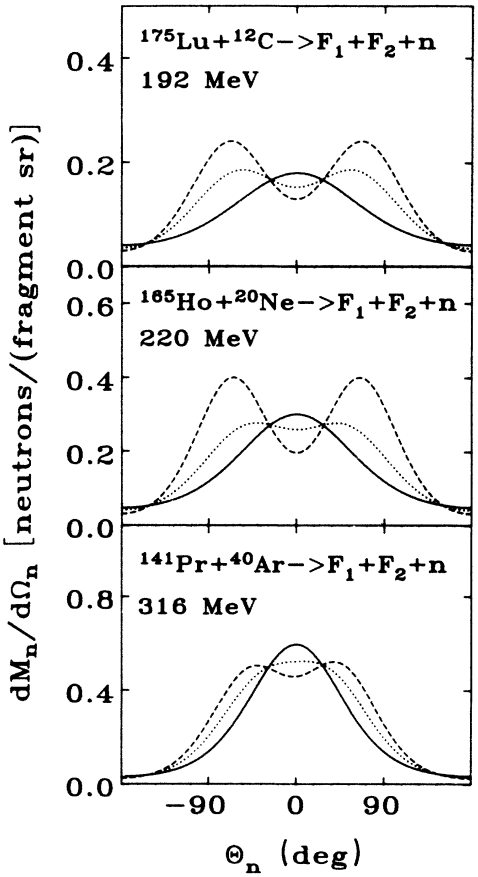

FIG. 16. Neutron angular correlations calculated for neutron evaporation from fission fragments at various total kinetic energies (TKE) achieved during acceleration in the mutual Coulomb field. The calculations are made for symmetric trigger angles according to the experimental situations and the neutron energies are integrated between 2 and 10 MeV. Solid line: TKE=0 MeV; dotted line: TKE=40 MeV; dashed line: TKE=80 MeV.

Therefore we have to consider neutron evaporation during the transition time τ_{trans} to the scission point from an assumed transition state configuration. This additional neutron yield is not taken into account by the statistical code JULIAN which considers only the competition between different decay modes and does not include any dynamics.

To get an estimate on the number of neutrons evaporated during τ_{trans} we continued the evaporation calculation without fission using the excitation energy and spin of the nucleus after the emission of the mean prefission neutrons, protons, and α particles. On the way to the scission configuration the deformation of the composite system is a function of time. Here we approximated these time dependent deformations by the mean values $d=c/a$ obtained from the spin independent K_0^2 of the fission-fragment angular distributions as discussed in Sec. III. The resulting deformation energies[42] of 12.9, 14.5, and 15.6 MeV for the three systems Pr + Ar, Ho + Ne, and Lu + C, respectively, were subtracted from the mean total excitation energies and the rotational energies were computed for spheroids with $d=c/a$. From the statistical model calculations the number of neutrons $M_n^{trans}(\tau_{trans})$ emitted during the transition time τ_{trans} was obtained as well as the thermal excitation energy $E_S^*(\tau_{trans})$ at the scission configuration, both as a function of τ_{trans}. Then $E_S^*(\tau_{trans})$ was used to compute the average number of neutrons $M_n^{acc}(\tau_{trans})$ emitted from both fragments during the initial acceleration time $(1-3)\times10^{-21}$ s, taking into account different mass splits. In Fig. 17 $M_n^{prefiss}$, $M_n^{trans}(\tau_{trans})$, and $M_n^{acc}(\tau_{trans})$ are plotted versus the transition time τ_{trans}. The intersection of the heavy solid line, representing the sum $M_n^{prefiss}+M_n^{trans}(\tau_{trans})+M_n^{acc}(\tau_{trans})$ with the experimentally observed prescission multiplicity (EXP) then yields the transition time τ_{trans}.

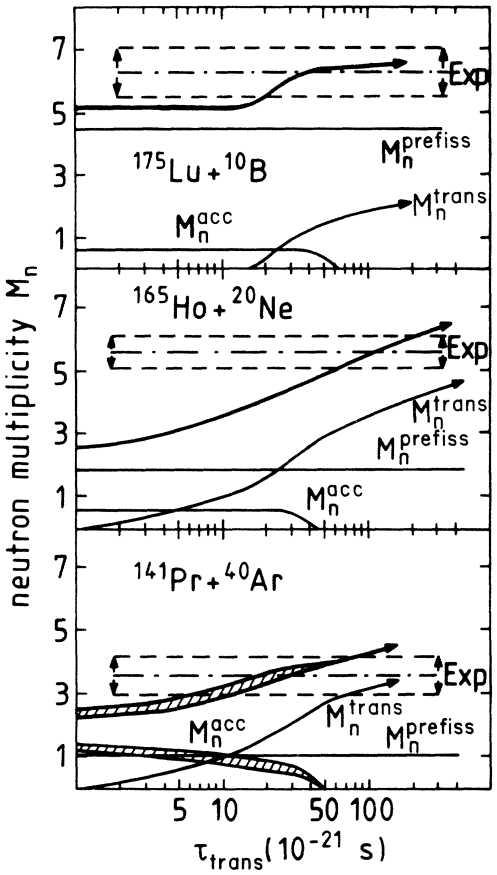

FIG. 17. Comparison between the experimental prescission neutron multiplicities (EXP) and statistical model calculations as a function of the transition time τ_{trans} to the scission point: $M_n^{prefiss}$ represents prefission neutrons, M_n^{trans} represents evaporated neutrons during the transition to the scission point, and M_n^{acc} represents neutrons evaporated from separated but not fully accelerated fission fragments. The heavy solid line represents the sum of all calculated components.

The results of the comparison between experiment and calculation are given in Table VII. The deduced transition times to the scission point are unexpectedly large and will be interpreted in Sec. IV B. The total neutron multiplicities M_n^{FF} of the fission fragments (FF) after separation were also calculated with JULIAN assuming that the thermal excitation energy $E_S^*(\tau_{trans})$ at the deduced transition times τ_{trans} is apportioned according to the mass numbers of the fragments. Agreement with the measured postscission neutrons is achieved if the experimental value is increased by the calculated number of neutrons M_n^{acc} emitted during the first stages of acceleration of both fission fragments. The value of $\frac{1}{2}M_n^{acc}$ is 0.4, 0.0, and 0.0 for the systems Pr + Ar, Ho + Ne, and Lu + C, respectively. The total neutron multiplicities for the evaporation residues also agree quite well with the experimentally measured ones.

In summary, we have deduced under the given assumptions the transition times of an iridiumlike composite system from a transition-state configuration with a maximum spin of 109$\hbar$, 94$\hbar$, and 62$\hbar$ to the scission point to be larger than 0.8, 6, and 2×10^{-20} s, respectively. As one would expect, the system with highest spin shows the shortest transition time.

B. Interpretations of the long transition times to the scission point

The comparison of the large experimental prescission neutron multiplicities with statistical model calculations, taking into account the neutron emission of the composite system on its way to scission and the emission from not fully accelerated fission fragments after separation, results in long transition times to the scission point of $(2-11)\times10^{-20}$ s. These very long transition times can be explained possibly by large nuclear viscosity[11,43-48] of the highly excited nuclei. To investigate this possibility we assumed a two-body friction process and Rayleigh dissipation[44] according to Davies *et al.*[43] Due to nucleon-nucleon collisions kinetic energy of the collective motion of the system moving to the scission point is transferred into internal excitation energy causing the system to slow down and increasing the temperature on its way to the scission point. The total energy dissipated from the transition state configuration to the scission configuration is directly proportional[44] to the two-body viscosity coefficient μ.

For a viscous system the transition time can be very

TABLE VII. Calculated parameters with the modified code JULIAN and comparison with the experimental results. Used parameters: Fermi-gas level densities $a=A/10$, $a_f/a_n=1.0$, $B_F=0.8B_F^{\mathrm{RLDM}}$.

Reaction	Statistical model					Experiment	
	M_n^{prefiss} (neutrons)	τ^{prefiss} [b] (10^{-21} s)	τ^{presc} [c] (10^{-21} s)	M_n^{FF} [e] (neutrons)	M_n^{ER} (neutrons)	M_n^{presc} (neutrons)	M_n^{FF} [e] (neutrons)	M_n^{ER} [f] (neutrons)
Pr + Ar	1.1	4.1	27^{+70}_{-15}	2.68(−0.4)[d]	8.0	3.6±0.6	2.2 ±0.2	7.86±0.09
Ho + Ne[g]	1.9	5.5	120^{+90}_{-50}	1.93	9.6	5.6±0.5	1.85±0.35	10.36
Lu + C[a]	4.5	34.0	80^{+-}_{-30}	1.85	9.9	6.3±0.8	1.8 ±0.3	9.14±0.07

[a] Calculated for ^{175}Lu + ^{10}B at $E_{\mathrm{lab}}=159$ MeV to take into account incomplete fusion.
[b] Lifetime of the system up to the point of fission decision.
[c] Total lifetime of the system up to the scission point.
[d] For comparison with experiment the number of neutrons (given in parentheses) emitted during the acceleration of fission fragments has to be subtracted (see the text).
[e] Per fission fragment.
[f] Measured with the 4π scintillator tank.
[g] Reference 3.

large[42,43] and the scission configuration can become very elongated compared to a nonviscous one as shown for the ^{236}U nucleus.[43–45] By assuming such a two-body friction process it is possible to determine the viscosity parameter μ which can be expressed in the unit terapoise,

$$1\ \mathrm{TP}=10^{12}\ \mathrm{P}=10^{12}\ \mathrm{dyn\,s/cm^2}$$
$$=6.24\times10^{-22}\ \mathrm{MeV\,s/fm^3}\ .$$

The transition time τ_{trans} to the scission point can be calculated as a function of the two-body viscosity parameter μ in a macroscopic model[43] as done for the system ^{236}U. From this system we take the almost linear relation between the viscosity coefficient and the transition time τ_{trans}. Davies *et al.*[43] have shown that the dissipated energy for systems with fissility parameters of about $x=0.65$ and for a viscosity parameter $\mu\approx0.01$ TP is approximately $E_{\mathrm{dis}}\approx0.012E_s^0$, with E_s^0 being the surface energy of a spherical nucleus which results in $E_{\mathrm{dis}}\approx3$ MeV. Assuming a linear dependence of the dissipated energy E_{dis} on μ up to $\mu=0.15$ TP and transfer of the dissipated energy into internal thermal excitation energy, one has to increase the temperature of the mean fissioning nucleus in the statistical model calculation as a function of τ_{trans} correlated with the viscosity parameter μ. We approximated the time dependent increase of the excitation energy up to the

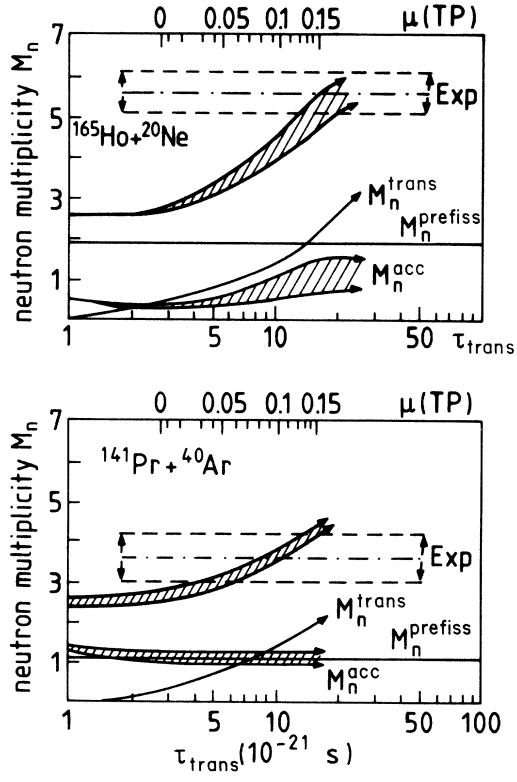

FIG. 18. Comparison between the experimental prescission neutron multiplicities (EXP) and statistical model calculations taking into account the effect of energy dissipation according to a two-body friction process.

TABLE VIII. Deduced parameters with the statistical model code JULIAN taking into account two-body viscosity effects and comparison with the experimental results. For used parameters, see Table VII. (Note that footnote indicators b–e refer to Table VII.)

	Statistical model					Experiment	
Reaction	$M_n^{prefiss}$ (neutrons)	$\tau^{prefiss}$ [b] (10^{-21} s)	τ^{presc} [c] (10^{-21} s)	μ (TP)	M_n^{FF} [e] (neutrons)	M_n^{presc} (neutrons)	M_n^{FF} [e] (neutrons)
Pr + Ar	1.1	4.1	14^{+8}_{-5}	$0.09^{+0.07}_{-0.06}$	2.71(−0.5)[d]	3.6±0.6	2.2 ±0.2
Ho + Ne	1.9	5.5	26^{+20}_{-7}	≥ 0.13	1.92(−0.5)[d]	5.6±0.5	1.85±0.35

scission point configuration by adding half of the total dissipated energy E_{dis} to the mean excitation energy of the fissioning nucleus.

In contrast to a nonviscous system, the temperature of fission fragments is not necessarily lower for larger transition times τ_{trans} if the added dissipation energy E_{dis} is larger than the cooling by particle evaporation with increasing τ_{trans}, and thus there is a larger contribution to the prescission neutron multiplicity by the neutron emission from not fully accelerated fission fragments. The results of the statistical evaporation calculation with the modified excitation energy $E_S^*(\tau_{trans})$ for Pr + Ar and Ho + Ne are shown in Fig. 18 and given in Table VIII. Due to the additional thermal excitation energy dissipated by the two-body friction process the fissioning nuclei evaporate neutrons and charged particles faster than nonviscous nuclei. The extracted transition times of $(1-2)\times 10^{-20}$ s for Pr + Ar and Ho + Ne, respectively, however are related with very large two-body viscosity coefficients μ of about 0.1 TP. This coefficient is seven times larger than determined by Davies *et al.*[43] As shown in Table VIII the total neutron multiplicities of the fission fragments after separation are in reasonable agreement with the experimental ones.

We also compared our results with a model developed by Hassani and Grangé[46] and Grangé.[27] In this model the fission process is considered to be a phenomenon of diffusion with respect to the fission degree of freedom. For high temperatures and angular momenta no potential pocket is assumed to be significant anymore and the entire fission process is considered to be predominantly by a transient phenomena.[10,47] Here we consider the case for which the potential pocket is nonexistent. The collective potential can then be described by an inverse parabola $V(x) = -\frac{1}{2}\mu_R\omega_0^2 x^2$ where μ_R is the reduced mass of the composite nucleus and ω_0^2 is the curvature of the harmonic oscillator potential. We then assumed that the transition time $\tau_{trans} \approx 1\times 10^{-20}$ s, as extracted for the system Pr + Ar under the assumption of pure two-body dissipation, can be approximated by the time t_0 in formula (2-23) in Ref. 47. In this formula t_0 is the time for which the fission process starts to be governed essentially by the collective potential of the composite system. The time is strongly dependent on the value of ω_0. For instance, by using $t_0 = 1\times 10^{-20}$ s and $\hbar\omega_0 = 1.5$ or 0.8 MeV we obtain a friction parameter of $\beta = 18\times 10^{21}$ s^{-1} or 4×10^{21} s^{-1}, respectively. The parameter β is the ratio of the two-body viscosity coefficient and the collective mass. These two examples show clearly the strong dependence of β on the curvature of the oscillator potential which unfortunately is not known.

In summary, we have studied transition times to the scission point and two-body viscosity coefficients of highly excited iridiumlike composite systems. Transition times of $>5\times 10^{-21}$ s have been deduced by comparing measured prescission neutron multiplicities with statistical model calculations taking into account pure two-body dissipation mechanisms during the transition to scission. The correlated viscosity coefficients are larger than at least 0.03 TP. The average of the deduced viscosity coefficient of about 0.1 TP, however, is seven times larger

than the value calculated by Davies *et al.*[43] from total kinetic energies of fission fragments. This discrepancy might be solved by the additional consideration of one-body dissipation mechanisms.[45,49] Our main purpose was to demonstrate the effect of a large dissipation of collective motion into internal excitation energy on the prescission neutron multiplicity. The additional heating decreases the emission times and consequently reduces all deduced transition times to the scission point.

V. CONCLUSIONS

We have measured and investigated fission-fragment angular distributions and neutron emission in coincidence with evaporation residues and fission events in the reactions Pr + Ar and Lu + C at 316 MeV argon and 192 MeV carbon bombarding energy. The results are compared with those obtained by the analysis of the previously measured reaction Ho + Ne (Refs. 3 and 20) at 220 MeV neon bombarding energy. All reactions are leading to comparable composite systems with similar total excitation energies.

From the analysis of the measured angular distribution of evaporation residues and fission fragments of the reaction Pr + Ar and Lu + C the angular momentum window contributing to fission was deduced to be 50–109 $\hbar$ and 49–62 $\hbar$, respectively. Together with the previously investigated system Ho + Ne, where this window is 57–94 $\hbar$, it was possible to study the dynamics of fission as a function of the spin of the composite system.

In order to obtain detailed information about the dynamical behavior of fissioning composite systems, we investigated the prescission and postscission neutron emission in coincidence with fusion-fission events in all three reactions characterized by different entrance-channel mass asymmetries. The different mass asymmetries are correlated with different formation times of the composite systems giving one the possibility to examine these times by looking for emitted neutrons originating from the fusion phase of the reaction. A comparison between the measured prescission neutron multiplicities and statistical model calculations seems to indicate that there is no considerable neutron emission during the formation. This would mean that the formation times are short compared to the decay times and that all observed prescission neutrons are emitted by the composite system after relaxation of the mass asymmetry. In the reaction Lu + C we observed highly energetic neutrons in coincidence with fusion-fission events which are emitted during an early preequilibrium phase.[3] In contrast to the low energetic neutron evaporation from fully equilibrated systems, a strong anisotropy of the preequilibrium neutron emission with respect to the reaction plane was observed. It was shown that the number of neutrons emitted from both fission fragments during the acceleration phase in their mutual Coulomb field[3,5] and misinterpreted experimentally as prescission neutrons is smaller than one. Furthermore, statistical model calculations predict small numbers of prefission neutrons (neutrons emitted up to the time at which the system "decides" to fission) of 1.1, 1.9, and 4.5 compared to experimental measured ones of 3.6±0.6, 5.6±0.5, and 6.3±0.8 for the three reactions Pr + Ar, Ho + Ne, and Lu + C, respectively. We assumed that the remaining neutrons are emitted on the way to the scission-point configuration and consequently are giving information about the dynamics of the fission process. In order to reproduce these additional neutrons with a statistical evaporation code it was possible to deduce the transition time of iridiumlike composite systems from a transition configuration to the scission point. This time was found to be larger than 0.8, 6, and 2×10^{-20} s for fission from maximum spin values of 109$\hbar$, 94$\hbar$, and 62$\hbar$, respectively. As one would expect the highest spin shows the smallest transition time. The deduced respective mean values are found to be very large: 2.3, 11, and 5×10^{-20} s, however with large error bars (Table VII).

By comparing these long transition times with dynamical calculations made for the fissioning ^{236}U nucleus[43,44] under the assumption of pure two-body friction, we extracted very large two-body viscosity coefficients of about $\mu\approx0.1$ TP. These two-body viscosity coefficients are about a factor of 7 larger than those determined by Davies *et al.*[43] from the analysis of total kinetic energies of fission fragments. For such high viscosity coefficients the total kinetic energies would decrease by about 20 MeV due to the very elongated scission configuration as shown in Refs. 36 and 43. This discrepancy can probably be solved by assuming not only a pure two-body viscosity but a mixture of a relative small two-body and a large one-body friction.[11,45,49] One-body friction due to collisions between nucleons and the moving wall of the nucleus leads to a more compact scission configuration and consequently to larger total kinetic energies of the fission fragments.[11,45]

As a conclusion we can say that the large prescission neutron multiplicities observed in all three reactions can be understood as a result of long transition times to the scission point due to a large dissipation of collective energy into internal excitation energy of the fissioning nuclei. However, it would be premature to claim that this is a proof for a strong dissipation mechanism of the fissioning nucleus on its way to scission. There are probably some other possibilities for one to interpret the experimental observations.[50] The present data should stimulate further activities in understanding the experimental results.

[1]D. Hilscher, E. Holub, U. Jahnke, H. Orf, and H. Rossner, in *Proceedings of the Third Adriatic Europhysics Study Conference, Hvar, Yugoslavia, 1981,* edited by N. Cindro, R. A. Ricci, and W. Greiner (North-Holland, Amsterdam, 1981), p. 225.

[2]A. Gavron, J. R. Beene, B. Cheynis, R. L. Ferguson, F. E. Obenshain, F. Plasil, G. R. Young, G. A. Petitt, R. Jääskeläinen, D. G. Sarantites, and C. F. Maguire, Phys. Rev. Lett. **47**, 1255 (1981); **48**, 835(E) (1982).

[3]E. Holub, D. Hilscher, G. Ingold, U. Jahnke, H. Orf, and H. Rossner, Phys. Rev. C **28**, 252 (1983).

[4]D. Ward, R. J. Charity, D. J. Hinde, J. R. Leigh, and J. O.

Newton, Nucl. Phys. **A403**, 189 (1983).
[5]D. J. Hinde, R. L. Charity, G. S. Foote, J. R. Leigh, J. O. Newton, S. Ogaza, and A. Chatterjee, Phys. Rev. Lett. **52**, 986 (1984); **53**, 2275(E) (1984).
[6]L. Schad, H. Ho, G.-Y. Fan, B. Lindl, A. Pfoh, R. Wolski, and J. P. Wurm, Z. Phys. A **318**, 179 (1984).
[7]D. Logan, H. Delagrange, M. F. Rivet, M. Rajagopalan, J. M. Alexander, M. Kaplan, M. S. Zisman, and E. Duek, Phys. Rev. C **22**, 1080 (1980).
[8]H. Delagrange, D. Logan, M. F. Rivet, M. Rajagopalan, J. M. Alexander, M. S. Zisman, M. Kaplan, and J. W. Ball, Phys. Rev. Lett. **43**, 1490 (1979).
[9]C. Grégoire, C. Ngô, and E. Remaud, Nucl. Phys. **A383**, 392 (1982).
[10]P. Grangé, Li Jun-Qing, and H. A. Weidenmüller, Phys. Rev. C **27**, 2063 (1983).
[11]A. J. Sierk and J. R. Nix, Phys. Rev. C **21**, 982 (1980).
[12]H. Feldmeyer, Proceedings of the International School of Physics "Enrico Fermi" Course 87 on Nuclear Structure and Heavy-Ion Dynamics, Varenna, Italy, 1982.
[13]J. Tõke, R. Bock, G. X. Dai, A. Gobbi, S. Gralla, K. D. Hildenbrand, J. Kuzminski, W. F. J. Müller, A. Olmi, H. Stelzer, B. B. Back, and S. Bjornholm, Nucl. Phys. **A440**, 327 (1985).
[14]E. Cheifetz, Z. Fraenkel, J. Galin, M. Lefort, J. Péter, and X. Tarrago, Phys. Rev. C **2**, 256 (1970).
[15]Z. Fraenkel, I. Mayk, J. P. Unik, A. J. Gorski, and W. D. Loveland, Phys. Rev. C **12**, 1809 (1975).
[16]J. R. Birkelund L. E. Tubbs, J. R. Huizenga, J. N. De, and D. Sperber, Phys. Rep. **56**, 107 (1979).
[17]P. Fröbrich, Phys. Rep. **116**, 337 (1984).
[18]R. A. Cecil, B. D. Anderson, and R. Madey, Nucl. Instrum. Methods **161**, 439 (1979).
[19]U. Jahnke, G. Ingold, D. Hilscher, H. Orf, E. A. Koop, G. Feige, and R. Brandt, in *Proceedings of the Symposium Commemorating the 100th Anniversary of Hans Geiger's Birth, Berlin, 1982,* edited by W. v. Oertzen (Springer, Berlin, 1983), in Lecture Notes in Physics **178**, 179 (1983).
[20]H. Rossner, D. Hilscher, E. Holub, G. Ingold, U. Jahnke, H. Orf, J. R. Huizenga, J. R. Birkelund, W. U. Schröder, and W. W. Wilcke, Phys. Rev. C **27**, 2666 (1983).
[21]B. B. Back, R. R. Betts, K. Cassidy, B. G. Glagola, J. E. Gindler, L. E. Glendenin, and B. D. Wilkins, Phys. Rev. Lett. **50**, 818 (1983).
[22]R. Vandenbosch and J. R. Huizenga, *Nuclear Fission* (Academic, New York, 1973).
[23]M. Prakash, V. S. Ramamurthy, S. S. Kapoor, and J. M. Alexander, Phys. Rev. Lett. **52**, 990 (1984).
[24]S. Cohen, F. Plasil, and W. J. Swiatecki, Ann. Phys. (N.Y.) **82**, 557 (1974).
[25]J. R. Huizenga, J. R. Birkelund, L. E. Tubbs, D. Hilscher, U. Jahnke, H. Rossner, B. Gebauer, and H. Lettau, Phys. Rev. C **28**, 1853 (1983).
[26]M. Lefort, Z. Phys. A **299**, 47 (1981).
[27]T. Ericson and V. Strutinsky, Nucl. Phys. **8**, 284 (1958).
[28]M. B. Tsang, C. B. Chitwood, D. J. Fields, C. K. Gelbke, D. R. Klesch, and W. G. Lynch, Phys. Rev. Lett. **52**, 1967 (1984).
[29]J. Wilczynski, K. Siwek-Wilczynska, J. van Driel, S. Gonggrijp, D. C. J. M. Hageman, R. V. F. Janssens, J. Lukasiak, and R. H. Siemssen, Phys. Rev. Lett. **45**, 606 (1980).
[30]B. G. Harvey and H. Homeyer (unpublished); Lawrence Berkeley Laboratory Report LBL-16882, 1983.
[31]W. Bohne, W. Galster, K. Grabisch, and H. Morgenstern, Nucl. Instrum. Methods **A240**, 145 (1985).
[32]D. Hilscher, E. Holub, G. Ingold, U. Jahnke, H. Orf, H. Rossner, W. U. Schröder, H. Gemmeke, K. Keller, L. Lassen, and W. Lücking, in *Proceedings of the Workshop on Coincident Particle Emission from Continuum States in Nuclei, Bad Honnef, 1984,* edited by H. Machner and P. Jahn (World-Scientific, Singapore, 1984), p. 268.
[33]M. Hillman and Y. Eyal (unpublished), modified by H. Rossner.
[34]F. Pühlhofer, Nucl. Phys. **A280**, 267 (1977).
[35]D. W. Lang, Nucl. Phys. **77**, 545 (1966).
[36]M. Beckermann and M. Blann, Phys. Rev. C **17**, 1615 (1978).
[37]D. Wilmore and P. E. Hodgson, Nucl. Phys. **55**, 673 (1964).
[38]F. G. Perey, Phys. Rev. **131**, 745 (1963).
[39]J. R. Huizenga and G. Igo, Nucl. Phys. **29**, 462 (1962).
[40]L. C. Vaz and J. M. Alexander, Z. Phys. A **318**, 231 (1984).
[41]J. Kasagi, B. Remington, A. Galonsky, F. Haas, J. J. Kolata, L. Satkowiak, M. Xapsos, R. Racca, and F. W. Prosser, Phys. Rev. C **31**, 858 (1985).
[42]R. W. Hasse, Ann. Phys. (N.Y.) **68**, 377 (1971).
[43]K. T. R. Davies, A. J. Sierk, and J. R. Nix, Phys. Rev. C **13**, 2385 (1976).
[44]R. Wieczorek, R. W. Hasse, and G. Süssmann, *Proceedings of the 3rd IAEA Symposium on the Physics and Chemistry of Fission, Rochester, New York, 1973* (International Atomic Energy Agency, Vienna, 1974) p. 523.
[45]J. Blocki, Y. Boneh, J. R. Nix, J. Randrup, M. Robel, A. J. Sierk, and W. J. Swiatecki, Ann. Phys. (N.Y.) **113**, 330 (1978).
[46]S. Hassani and P. Grangé, Phys. Lett. **137B**, 281 (1984).
[47]P. Grangé, Nucl. Phys. **A428**, 37c (1984).
[48]J. R. Nix, A. J. Sierk, H. Hofmann, F. Scheuter, and D. Vautherin, Nucl. Phys. **A424**, 239 (1984).
[49]J. W. Negele, S. E. Koonin, P. Möller, J. R. Nix, and A. J. Sierk, Phys. Rev. C **17**, 1098 (1978).
[50]H. Delagrange, C. Grégoire, F. Scheuter, and Y. Abe, Ganil report (unpublished).